ELSEVIER

Precision Engineering
Journal of the International Societies for Precision Engineering and Nanotechnology
24 (2000) 251–263

PRECISION ENGINEERING

Evaluation of circularity from coordinate and form data using computational geometric techniques

G.L. Samuel, M.S. Shunmugam*

Manufacturing Engineering Section, Department of Mechanical Engineering, Indian Institute of Technology, Madras-600 036, India

Received 7 July 1999; revised 10 November 1999; accepted 23 February 2000

Abstract

Data for evaluating circularity error can be obtained from coordinate measuring machines or form measuring instruments. In this article, appropriate methods based on computational geometric techniques have been developed to deal with coordinate measurement data and form data. The computational geometric concepts of convex hulls are used, and a new heuristic algorithm is suggested to arrive at the inner hull. Equi-Distant (Voronoi) and newly proposed Equi-Angular diagrams are employed for establishing the assessment features under different conditions. The algorithms developed in this article are implemented and validated with the simulated data and the data available in the literature. © 2000 Elsevier Science Inc. All rights reserved.

Keywords: Circularity evaluation; Minimum zone; Function-oriented; Computational geometry; Equi-Distant and Equi-Angular diagrams

1. Introduction

Present day engineering components need closer dimensional and geometric tolerances to achieve high levels of functional performance in the assemblies where they are used. Computer-aided manufacturing procedures have made it possible to produce the parts to satisfy the specified tolerances. It is imperative that the manufactured components be verified using compatible inspection machines and procedures to check their conformance to the design specifications. Computer-aided inspection (CAI) procedures capable of achieving high levels of performance in predicting the errors have gained popularity in recent years. To produce the desired results of inspection, data obtained from inspection devices must be analyzed using appropriate computer-based algorithms, and these algorithms must follow the specifications laid down in the standards. Moreover, these algorithms must be efficient, robust, and should consume optimal time for producing the results. In the past decade, the computational geometric techniques have attracted enormous attention from designers of algorithms for solving geometric problems. These computational geometry-based algorithms can be applied for evaluation of form errors in the manufactured components.

The ANSI Dimensioning and Tolerance Standard Y14.5 specifies that the form tolerances on a component must be evaluated with reference to an ideal geometric feature [1]. ISO Standards recommends a minimum zone evaluation of form and specifies that the ideal/reference features must be established from the actual measurement data such that the deviation between it and the actual feature concerned will be the least possible value [2]. However, neither of these standards specifies the methods for establishing the ideal feature and evaluation of form errors.

Various researchers have attempted to develop methods for establishing the reference feature and to evaluate the circularity error. Least-squares method (LSM) is based on sound mathematical principles that minimize the sum of the squared deviations of the measured points from the fitted feature [3, 4]. This method is robust, but it does not follow the standards intently and will not guarantee the minimum zone solution specified in the Standards. In addition, the deviation values and geometric tolerances that are determined by LSM will be generally larger than the actual ones, and this may lead to rejection of good parts. The normal least-squares fit has also been tried by Murthy and Abdin [5]. To solve the

* Corresponding author. Tel.: +011-91-44-445 8520; fax: +011-91-44-235-0509; E-mail: shun@acer.iitm.ernet.in (M.S. Shunmugam).

PII: S0141-6359(00)00039-8

equations of normal least- squares fit, very tedious mathematical calculations and trial-and-error procedures are required. To obtain the minimum zone solution, the numerical methods based on Monte Carlo, Simplex and Spiral Search [5] and Simplex linear programming [6], have been adopted.

Shunmugam [3] has suggested a new simple approach called the median technique, which gives minimum value of circularity error. Using discrete Chebshev approximations, Danish and Shunmugam [7] have arrived at the minimum zone values.

Computational geometry-based techniques show greater promises for solving the minimum zone problems encountered in the geometrical evaluations. Techniques for dealing with datum-related features and definitions based on computational geometry have been given to formalize the meaning of geometric imperfections, according to the implications of the Standards [8]. Computational geometry-based assessment techniques for evaluation of roundness based on medial axis and Voronoi diagram methods have also been tried [9,10]. In a different attempt, a minimum zone center (MZC) based on the concept of Voronoi diagrams has been compared with least-squares center (LSC)[11].

It is also important that the measurement and evaluation of geometric errors should be carried out keeping in mind the functional requirements [12]. The function-oriented evaluation of engineering surfaces has greater practical significance, because the contact between the workpieces occurs at their extreme functional boundaries [8,13]. The importance of function-oriented evaluation in assembly and gauging has also been reported [14]. The concepts of ring gauge (minimum circumscribed) and plug gauge (maximum inscribed) centers are mentioned in the literature dealing with roundness assessment. However, very little attention has been given in the literature to the application of computational geometric techniques for the function-oriented form evaluation.

Coordinate data obtained using coordinate measuring machine (CMM) and form data obtained using roundness measuring instruments/setups have to be handled differently while evaluating the form errors. While analyzing the roundness data, it is necessary to account for distortion from size (radius) suppression and eccentricity in the measurement set-up. However, this aspect has been overlooked in some recent work reported in the literature, and it is found that the same algorithms have been applied for both types of data. In this article, appropriate methods are presented to deal with CMM data as well as form data. Minimum zone evaluation and function-oriented evaluation of circularity have been proposed on the basis of computational geometric techniques. Apart from such computational geometric concepts as outer hull (convex hull) and inner hull, the existing concept of Equi-distant (Voronoi) diagrams and newly introduced concept of Equi-angular (EA) diagrams are employed in this article. The results obtained using simulated data and the data reported in the literature are included in this article.

2. Evaluation of circularity error

In general, the circularity error is evaluated with reference to the assessment feature as [Eq. (1)]

$$\Delta = |e_{max}| + |e_{min}| \tag{1}$$

where $e_{\max}$ and $e_{\min}$ are the maximum and minimum deviations of the profile from the assessment feature. $e_{\max}$ is zero for minimum circumscribing feature, and the profile is inside this feature. $e_{\min}$ is zero in case of maximum inscribing feature, and the profile lies outside. For minimum zone evaluation, the deviation can be computed from any one of the assessment features enclosing the profile and having the least separation.

For CMM data shown in Fig. 1, the deviation of a point on the profile is given by [Eq. (2)]

$$e_i = [(x_i - x_0)^2 + (y_i - y_0)^2]^{1/2} - r_0 \tag{2}$$

where x_i and y_i are the coordinates of the point on the circular feature and (x_0, y_0) is the center of the assessment circle with radius r_0

For form data, the deviation is calculated from [Eq. (3)]

$$e_i = r_i - [r_0 + x_0 \cos\theta_i + y_0 \sin\theta_i] \tag{3}$$

where (r_i, θ_i) is the polar coordinate of the point on the circular profile. (x_0, y_0) is the center, and r_0 is the radius of the circle from which the limacon is obtained [15]. The details are discussed in a later section with reference to Fig. 5(a).

3. Algorithms for CMM data

3.1. Crest circle (minimum circumscribed circle)

Fig. 1 schematically shows the measurement datapoints and the profile of a circular feature. In reality, the deviations from circularity will be far less than those shown in the figure. The measurement data obtained from the machines such as CMM will be in Cartesian coordinates, and there will be no size suppression. Generally, the diameter of the components will be of the order of millimeters, and the circularity deviations will be in microns. The convex outer hull (outer hull) of given set of points in Euclidean space is the boundary of the smallest convex domain containing all the points of the set. A domain is said to be convex if, for any two points in the domain, the segment connecting them should be entirely contained in the domain [16]. Because the minimum circumscribed circle (MCC) will pass through the three vertices on the outer hull, it is prudent to construct an outer hull first. In this article, the outer hull is determined by

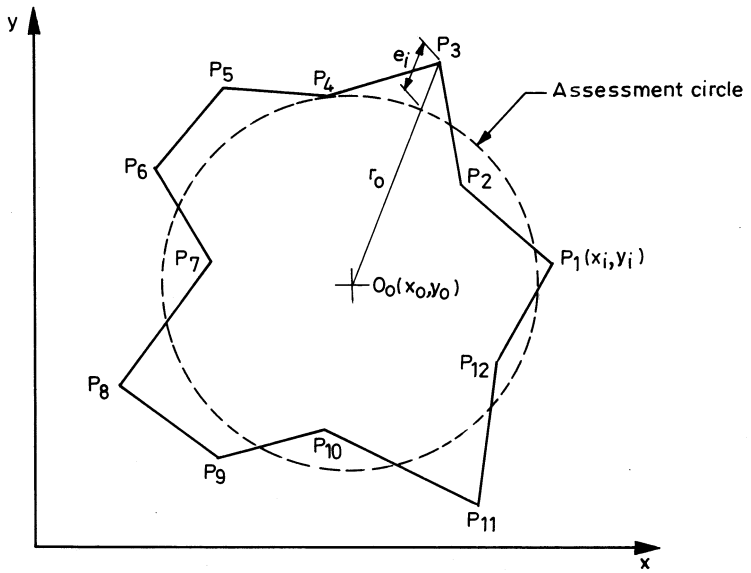

Fig. 1. CMM data of circular feature (x_i and y_i in mm)—for illustration only.

using "Divide and Conquer" and "Merge" technique suggested by Preparata and Hong [17]. This technique is very elegant and runs in optimal time.

Fig. 2(a) shows the outer hull with vertices V_1, V_2, etc. In the next step, equidistant (ED) lines, such as L_{12} L_{23}, and L_{34} are constructed for the edges V_1V_2, V_2V_3, and V_3V_4, respectively, as shown in Fig. 2(b). For example, L_{23} is the locus of the points equidistant from both the vertices V_2 and V_3. Let us further consider the line L_{23}. The line L_{23} intersects with L_{12} of the previous edge V_1 V_2, and L_{34} of the next edge V_3 V_4 at C_n and C_f, respectively. The intersection point C_f, which is farthest from the edge V_2 V_3 is the farthest center (C_{23}). A circle can be drawn with this as center and passing through V_2 and V_3. The portion of the line L_{23} beyond C_f, away from the edge V_2 V_3 is the farthest ED edge corresponding to the edge V_2 V_3 (FE_{23}). The concepts of Equi-Distant line and the farthest edge are explained in Appendix A. Following the procedure outlined in this section, the farthest ED edges corresponding to all the edges of the outer hull are constructed. It is seen from Fig. 2(b) that a few edges have common farthest centers. For example, farthest edges FE_{23} and FE_{34} have C_{23} and C_{34} as their centers, and for any point in the region enclosed by these two edges, the vertex V_3 will be the farthest. The outer hull is, therefore, updated by dropping the vertex V_3. Similarly, the vertices V_1 and V_6 are dropped, and a new hull is formed as shown in Fig. 2(c). New farthest ED edges are formed for this updated hull following the same procedure. In the next updating, the vertices V_4 and V_7 get dropped and only vertices V_2 and V_5 would remain. The equidistant line for these two vertices would pass through the common centers; namely, C_{72}, (C_{57}), and C_{24}, (C_{45}). The new edges FE_{24}, FE_{57}, and FE_{72} pass through the common centers of the initial hull and, therefore, would end at these common centers, as shown in Fig. 2(d). The completed diagram is also referred to as farthest Voronoi diagram in the computational geometry literature. By taking the centers of the completed ED diagrams, a number of circumscribing circles can be drawn for the given dataset. Out of these circles, one having the least radius is the Minimum Circumscribed or Crest Circle, as shown in Fig. 2(d). It should also be noted that MCC passes through V_2, V_5, and V_7, and its center is actually the intersection of the perpendicular bisectors of the sides of the triangle formed by V_2, V_5, and V_7.

3.2. Valley circle (maximum inscribed circle)

The convex inner hull (inner hull) of a set of points in Euclidean space is the boundary of the largest empty subset of given points. The inner hull for given set of datapoints representing the profile of the circle is determined for constructing the nearest ED diagram. Roy and Zhang [10] suggested that different inner hulls can be constructed starting from different initial points, and the hull with maximum width can be selected. This leads to several trials and frequently ambiguous results are obtained. A new heuristic algorithm for finding inner hull is proposed in the present work. This method involves profile inversion, and the original data are transformed with reference to an assumed circle, as shown in Fig. 3(a). For this purpose, a suitable center is to be determined for the given set of datapoints. The MCC center obtained while evaluating the circularity error may be taken as a center. With this as center *O*, a suitable diameter of the circle is selected such that all the points on the profile are within this assumed circle. The transformation is done by plotting the radial deviations between the points on the original profile and the corresponding points on the assumed circle. For example, the point P_3' is obtained by marking along the radial line the distance *a* that represents the deviation P_3 S_3.

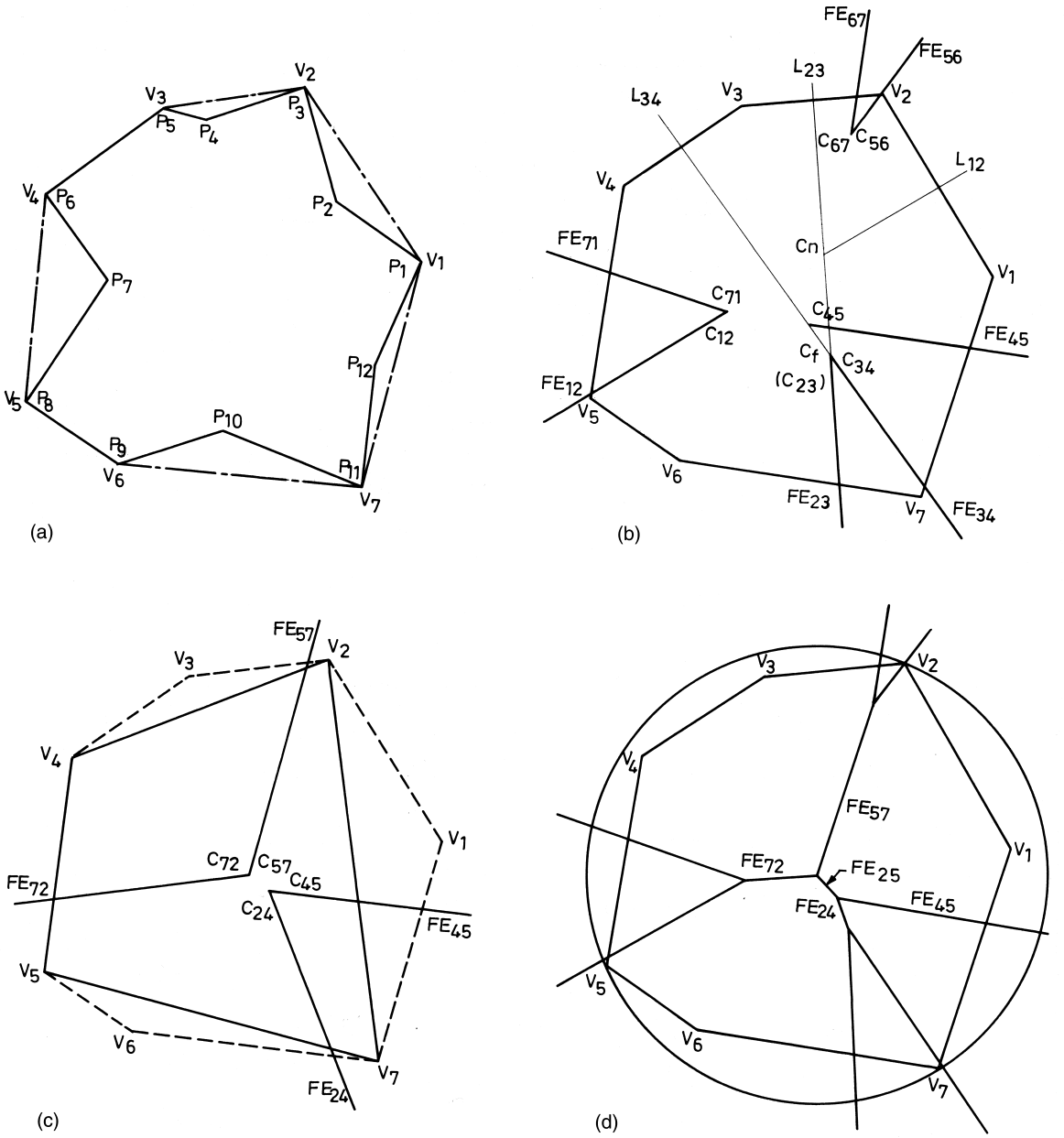

Fig. 2. Constuction of farthest ED diagram: (a) outer hull; (b)initial farthest ED edges; (c) updated hull and farthest ED edges; (d) farthest ED diagram and minimum circumscribed circle.

Mathematically, it is expressed as [Eq. (4)]

$$r_i' = r_a - r_i \tag{4}$$

where r_i' represents the radius of the points on inverted profile, r_a is the radius of the assumed circle, and r_i is the radius of the point on the original profile. Assuming a very large radius r_a can lead to considerable profile distortion. A simple heuristic rule to select the radius of this circle is [Eq. (5)]

$$r_a = r_{max} + \delta \tag{5}$$

where $\delta = k(r_{max} - r_{min})$, and k can be selected between 0.5 and 1.0. r_{max} and r_{min} are the maximum and minimum radii with respect to the selected center.

The convex outer hull for the transformed profile is determined as explained earlier. The points of the original dataset corresponding to the vertices of the outer hull of the transformed profile are taken as the vertices of the inner hull, as shown in Fig. 3(b) schematically. The procedure for constructing the nearest ED diagram is similar to that of the farthest ED diagram, except that the nearest intersection points are considered as end points of the nearest ED edges instead of farthest intersection points. Fig. 3(b) shows the

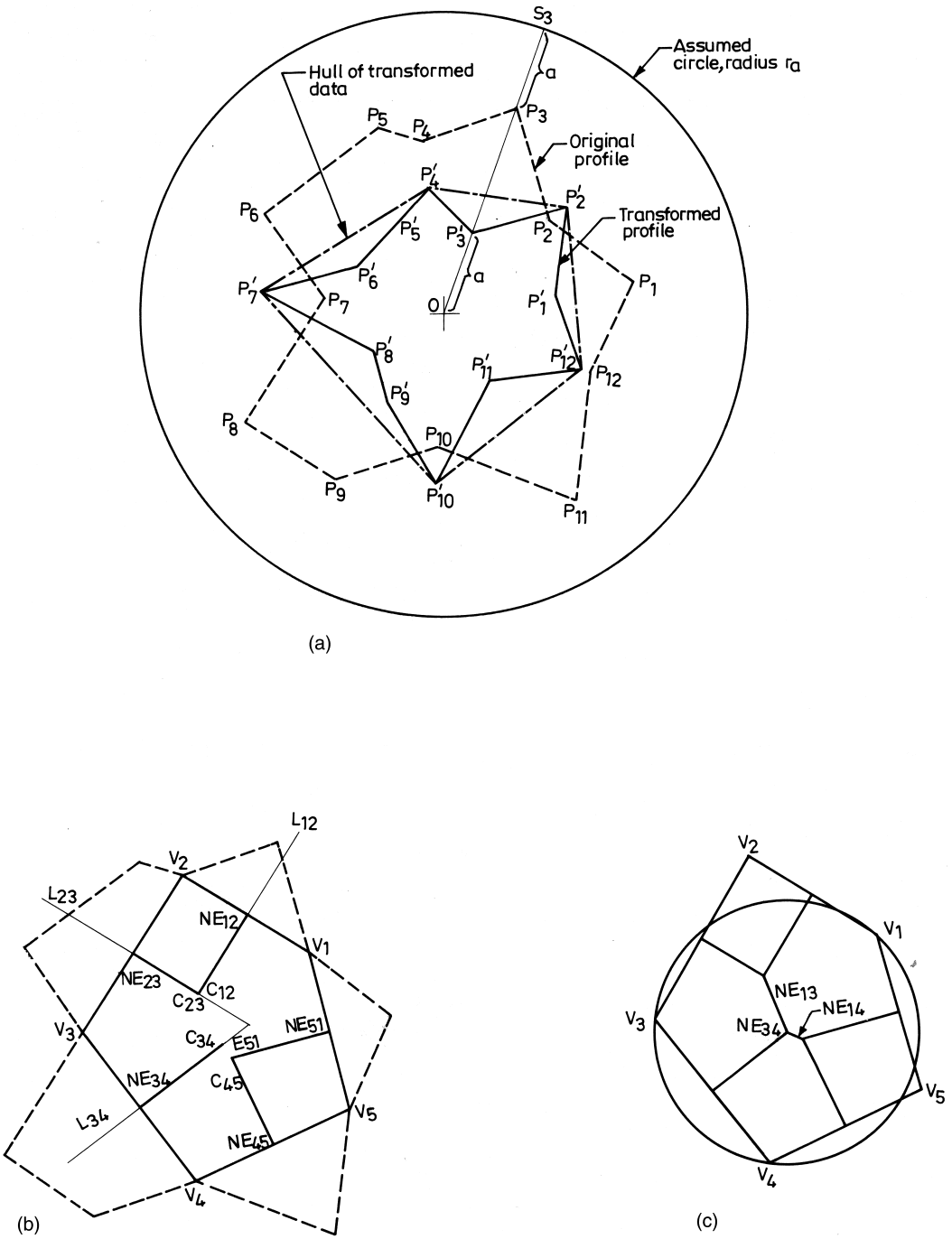

Fig. 3. Constuction of nearest ED diagram;(a) transformed data and its hull; (b) initial nearest ED edges; (c) nearest ED diagram and maximum inscribed circle.

nearest ED edges for the initial hull. The nearest ED edge for V_2 V_3 is obtained from the three ED lines; namely, L_{12}, L_{23}, and L_{34}. The nearest intersection point is taken as the nearest ED center C_{23}, and the ED line toward the edge V_2 V_3 from this nearest center is the nearest ED edge NE_{23}. The hull is updated by dropping the vertices that have common nearest ED centers. For example, the ED centers C_{12} and C_{23} are common, and hence the vertex V_2 is dropped. Fig. 3(c) shows the complete nearest ED diagram and the Maximum Inscribed Circle (MIC) or Valley circle.

3.3. Minimum zone circles

The minimum zone circles are obtained when two concentric circles contain all the points of the dataset and have minimum radial distance between them. To meet these criteria, the minimum zone circles should pass through at

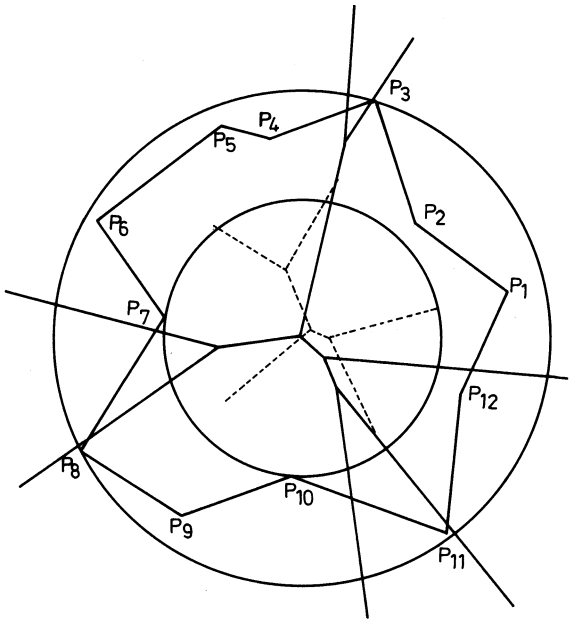

Fig. 4. Superimposed farthest and nearest ED diagrams along with MZC.

least four points of the dataset. This can occur when the three points lie on one circle and the fourth point on the other circle concentric to it or when two points are on each circle.

The farthest and nearest ED diagrams are superimposed, as shown in Fig. 4. The intersection points of these two diagrams are the candidate centers [9,10]. The smallest possible circumscribing circle and largest possible inscribing circle with center at the intersection points of farthest and nearest ED diagrams are established. Such circles will contain all the points of the dataset in between them. In case an intersection point coincides with a common center of either the farthest or nearest ED edges, one of circles would be controlled by three points. Otherwise, both circles are controlled by two points each. The radial distance between these concentric circles is found, and a pair having minimum radial separation gives the Minimum Zone Circles (MZC). Examination of Equation 2 would also reveal that a pair of concentric circles resulting in a minimum difference between the radius of the outer circle and that of the inner circle would be the MZC, and the minimum difference is the form error. It may be noted in Fig. 4 that the outer circle passes through two points, P_3 and P_8; whereas, the inner circle passes through P_7 and P_{10}.

4. Algorithms for form data

The form data will be different from CMM data, because there will be distortion from radius suppression and eccentricity in form measurement setup. The data obtained from the roundness measuring instruments/set-ups will be in the polar form, with the radial values in microns and the angles in degrees. Even when a truly circular workpiece is measured, if the axis does not coincide with axis of the rotating table of the measuring instrument, a noncircular profile is obtained. It has been proved in the literature that this profile can be approximated to a limacon and expressed in the linear form as [EQ. (6)]

$$R_i = r_0 + x_0 \cos\theta_i + y_0 \sin\theta_i \tag{6}$$

Therefore, the evaluation of the form data is carried out with reference to a limacon, because it is difficult to eliminate the setting error completely during the measurement.

4.1. Crest and valley features

Fig. 5 (a) shows the form data of the circular feature with uniform angular spacing. It also shows a limacon assessment feature and the manner in which the error is obtained with reference to this limacon. The relevant aspects of limacon are discussed in Appendix B. The outer hull is established for the form data also using “Divide and Conquer” and “Merge” techniques. The construction details further discussed here for form data relate to the EA concepts shown in Appendix A. At each vertex, a line is drawn perpendicular to the radial line joining the vertex and the center. Fig. 5(b) shows perpendicular lines L_1, L_2, L_3, etc. for vertices V_1, V_2, V_3, etc. At the intersection of these perpendicular lines; namely, I_{12}, I_{23}, I_{34}, etc., equi-angle (EA) lines are constructed as the angle bisectors. The concepts of the farthest center and the farthest edge are same as ED edges, but the circle with suitable radius drawn with farthest center on EA line will be tangential to the respective perpendicular lines. For example, the circle can be drawn with center C_{23} tangential to the lines L_2 and L_3. It should be noted that the circle being referred to here represents the circle from which the limacon is constructed. Fig 5(c) shows the complete farthest EA diagram along with the candidate centers for constructing the circles for establishing the circumscribing limacons. The smallest circle is chosen to obtain the Minimum Circumscribing Feature (MCF) or limacon. Fig 5(c) shows that the smallest circle thus obtained is tangential to the perpendicular lines at V_2, V_5, and V_7. In other words, the center of this circle is actually the intersection of the angle bisectors of the triangle formed by the three perpendicular lines. For the sake of understanding, the limacon established from this circle is also shown in Fig. 5(c), and this limacon passes through V_2, V_5, and V_7. This figure is given to illustrate the concepts involved. The application of these concepts to the actual data is discussed in the section on results and discussions.

The nearest EA diagram is constructed using the inner hull obtained based on the heuristic method explained earlier and the Maximum Inscribing Feature (MIF) or limacon is established from the largest circle obtained using the nearest EA diagrams.

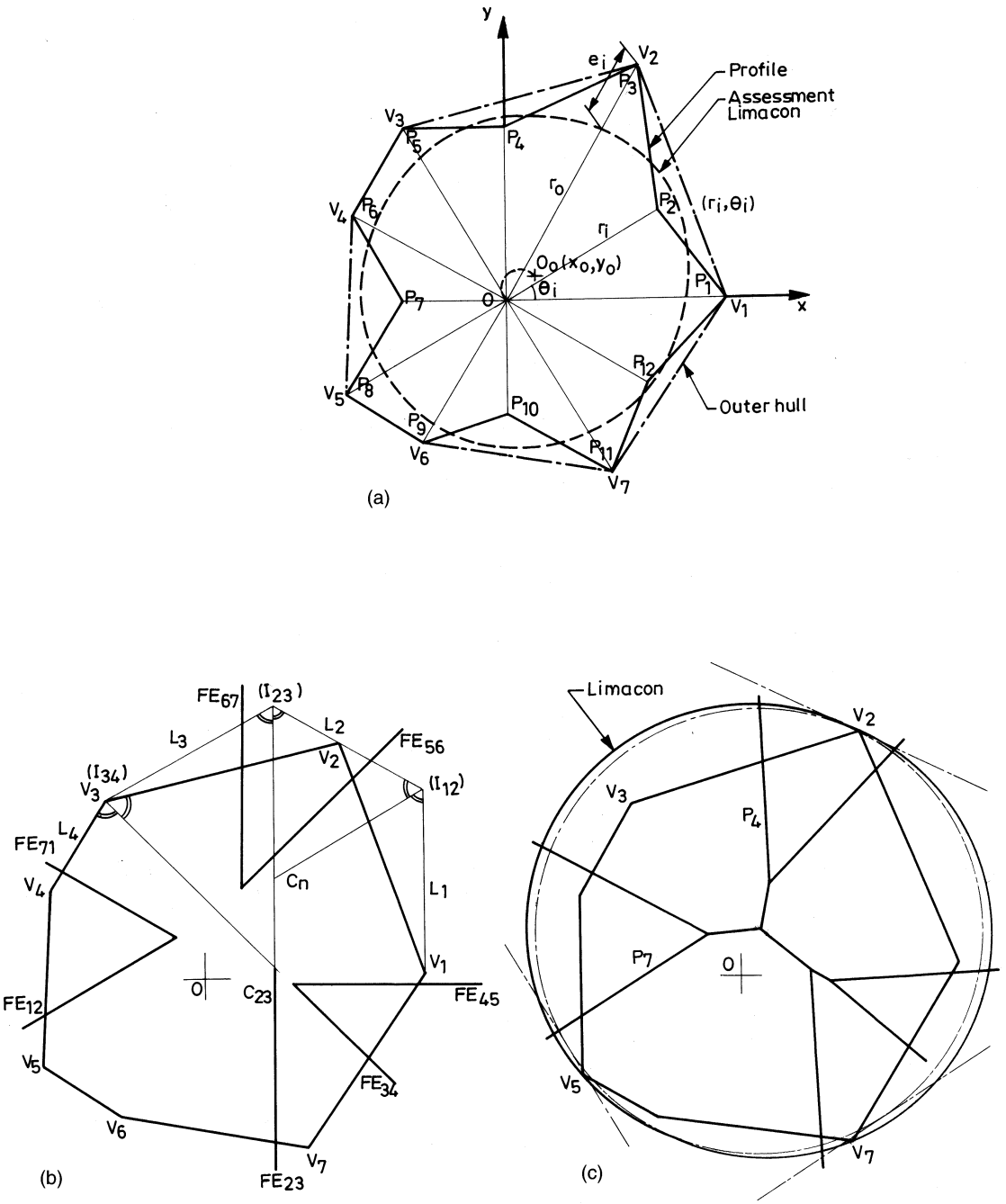

Fig. 5. Form data and farthest EA diagram: (a) form data (r_i in μm, θ_i in deg) (for illustration only); initial hull and farthest EA edges; (c) farthest EA diagram and minimum circumscribing Limacon.

4.2. Minimum zone features

The farthest and nearest EA diagrams are superimposed, and the intersection points are considered as the centers of the circles from which the limacons are established for form error evaluation. A pair of limacons giving minimum value of form error is identified as Minimum Zone Features. It is interesting to note that the difference between the radius values (r_0) of the outer and inner circles corresponding to the respective limacons denotes the minimum zone error. Examination of the Equation 3 would confirm this, as the centers (x_0, y_0) are same for both cases.

5. Results and discussion

Computer programs were written in C++ based on the proposed algorithms and run on Pentium, 233 MHz machine. The package was run for the data available in the literature and for the simulated data. The datasets are in-

cluded in Appendix C. The CMM dataset C1(a) is simulated from the form dataset C1(b) available in the literature [3]. Dataset C2(a) shows the CMM data [18], and dataset C2(b) shows the form data obtained by applying suitable transformations on dataset C2(a). The proposed algorithms work for data with both uniform and nonuniform spacing. Tables 1(a) and (b) shows the results of the function-oriented and minimum zone evaluation of circularity. The values obtained by the least-squares method are also included in the tables for comparison. The LSM is simple and straightforward, only when it is applied to form data with the deviations expressed as linear equation (Eq. 3). In case of CMM data, an appropriate search method [15] is used to minimize the sum of the squares of the normal deviations where the normal deviations are expressed by Eq. 2.

The datasets taken here serve as examples to bring out the differences in approaches to be followed for evaluating the CMM and form data. It should be remembered that the data obtained by the roundness measurement are characterized by the size suppression; whereas, the CMM data contain the size as well as the form information. The results show that the form error values, for a given circular feature, evaluated based on limacon in case of form data and circle in case of CMM data are the same. The CMM data given in Appendix C, dataset C1(a) are simulated from the form dataset given in dataset C1(b) and expressed up to eight decimal places. Generally, CMMs measure up to the third decimal place. Therefore, simulation was carried out by rounding off the values given in dataset C1(a) to the third and fourth decimal places. It was observed that MZ values of 2.003 μm and 2.235 μm were obtained, instead of an MZ value of 2.24264 μm obtained for form data.

It has also been observed in some recent works that the form dataset C1(b) has been treated like coordinate data

Table 1
Results of circularity evaluation

1(a): CMM Data (given in Appendix C)

Data	Parameters	Reported Method			Present Method			LSM
		MCC	MIC	MZ*	MCC	MIC	MZ*	
Set 1(a)	x_0 (mm)	—	—	—	40.0000	40.00000	39.9998	40.0002
	y_0 (mm)	—	—	—	30.0014	30.0010	30.0022	30.0012
	r_0 (mm)	—	—	—	25.0040	25.0020	25.0030	25.0030
	Δ (μm)	—	—	—	2.4147	2.2945	2.2430	2.4657
	Time (s)	—	—	—	0.049	0.049	0.098	0.649
Set 2(a)	x_0 (mm)	40.0005[18]	40.0016[18]	40.0008[18]	40.0005	40.0016	40.0007	40.0014
	y_0 (mm)	50.0015[18]	50.0003[18]	40.0016[18]	50.0015	50.0003	50.0015	50.000
	r_0 (mm)	30.0145[18]	29.9865[18]	30.0001[18]	30.0145	29.9865	30.0000	30.0005
	Δ (μm)	29.3630[18]	29.6270[18]	29.2860[18]	29.3541	29.61540	29.2816	29.7813
	Time (s)	0.03[18]	0.03[18]	0.05[18]	0.050	0.050	0.100	0.990

*Assessment feature having equal magnitude of maximum deviations on either side

1(b): Form Data (given in Appendix C)

Data	Parameters	Reported Method			Present Method			LSM
		MCF	MIF	MZ*	MCF	MIF	MZ*	
Set 1(b)	x_0 (μm)	0.000[3,18] 0.0752[10]	0.000[3,18] −0.2500[10]	0.000[3] −0.1280[10] −0.1213[18]	0.0000	0.0000	−0.12132	0.1465
	y_0 (μm)	1.414[3,18] 1.4330[10]	1.000[3,18,10]	1.000[3,10] 1.1213[18]	1.4142	1.000	1.1213	1.200
	r_0 (μm)	4.000[3,18] 4.1783[10]	2.000[3,18] 2.0156[10]	3.1465[3] 4.2474[10] 3.000[18]	4.0000	2.0000	3.0000	3.000
	Δ (μm)	2.414[3,18] 2.6095[9,10]	2.293[3,18] 2.3505[9,10]	2.293[3] 2.2433[9,10] 2.2426[18]	2.4142	2.2929	2.2426	2.455
	Time (s)	0.02[18]	0.01[18]	0.02[18]	0.059	0.060	0.119	0.009
Set 2(b)	x_0 (μm)	−6.200[18]	−5.1000[18]	−5.900[18]	−5.9433	−5.1229	−5.9602	−5.2984
	y_0 (μm)	10.600[18]	9.400[18]	10.700[18]	10.0263	9.4069	10.6228	9.1556
	r_0 (μm)	48.700[18]	20.700[18]	34.300[18]	48.7380	20.7026	34.2762	34.7609
	Δ (μm)	29.3625[18]	29.6269[18]	29.2864[18]	29.3501	29.6179	29.2809	29.7564
	Time (s)	0.03[18]	0.03[18]	0.05[18]	0.110	0.110	0.220	0.010

*Assessment feature having equal magnitude of maximum deviations on either side

and, interestingly, the minimum zone values obtained are closer [9,10]. This coincidence is a freak phenomenon, because the values obtained for the minimum circumscribing and maximum inscribing features show clearly the error introduced in ignoring the differences in the data. It is also found that by treating the form data as coordinate data, the parameters of the assessment features, such as x_0, y_0, and r_0 are also different (Table 1(b)).

The values of the center position and size obtained by LSM show considerable statistical stability, because all the measured points are included in the computation of these values. In case of MZ and function-oriented evaluation, the center position and size are determined by the extreme points. In the first instance, the features established by the extreme points may seem to have little practical significance. It should be remembered here that in any method used for establishing the assessment/reference features, the value of the circularity error is based on the extreme points only. Therefore, proper care must be exercised in all cases with regard to the unstable extreme points and uncertainty in their measurements. The size value r_0 is more significant in case of function-oriented evaluation, because it decides the size of the mating part during the assembly.

In the proposed algorithms, the convex outer hull and the inner hull of the given set of datapoints are taken so that most of the points that do not influence the final results are eliminated, and the construction of ED and EA diagrams becomes less cumbersome. To test the proposed method for datasets containing large number of points, simulation was carried out to arrive at MZ values for datasets with 100, 500, and 1,000 points, and the computation times of 0.21 s, 0.43 s, and 0.64 s, respectively were obtained. It can also be shown that if N represents the number of points in the dataset, the computational complexity of finding the convex outer hull by divide and conquer algorithm, is $O(N \log N)$. The complexity of finding inner hull is also $O(N \log N)$, because the time required for transforming the data is $O(N)$and for finding outer hull of the transformed data is $O(N \log N)$. The ED and EA diagrams can be constructed in $O(N \log N)$ time. Hence, the over-all complexity of the algorithms is $O(N \log N)$. For comparison with LSM, the computation times are also included in the Tables 1(a) and (b).

6. Conclusions

Considering the need for algorithms for processing geometric data in the modern measuring instruments, the algorithms for form evaluation based on computational geometric techniques have been developed in the present work. These techniques are elegant, because the geometrical aspects can be visualized much better than the mathematical aspects of the numerical techniques. The concept of Equi-distant and Equi-angular lines are more fundamental in nature and are quite useful in understanding the methods for establishing the assessment features. The minimum zone as well as function-oriented evaluations of circularity error have been carried out, and the results are presented. The proposed algorithms can handle data with both uniform and nonuniform spacing. The proposed method uses the concepts of convex hulls and a new heuristic approach for inner hull that gives unique results, thereby achieving considerable reduction of the computation times.

In some recent works on application of computational geometric approaches for evaluation circularity, the results have been reported treating the form data as coordinate data, ignoring their differences. These reported results show considerable variation from the actual values obtained by applying appropriate methods. While processing the CMM data, a circular assessment feature must be considered. The circular feature would pass through the selected datapoints. In case of form data, because the size is suppressed, and the axis of the inspected component and the measuring instrument would not coincide, a limacon feature must be considered. The limacon would pass through the selected datapoints. However, the circle from which the limacon is established would be tangential to the lines perpendicular to radial lines of the selected datapoints.

The present method for minimum zone evaluation always guarantees a minimum value for a given set of datapoints. Function-oriented form evaluation has many practical applications, because the contact between the parts in assembly will occur at the functional boundaries. In the present work, computational geometric approach has been extended for function-oriented evaluation of circularity, and the effectiveness of these techniques has been demonstrated successfully using the simulated data and the data reported in the literature. These algorithms are computationally less complex, quite robust giving unique solution and require short time for execution. They are well suited for the evaluation of form in form measuring instruments and CMMs. The present algorithms can not only be applied to full circular feature but also to the partial feature.

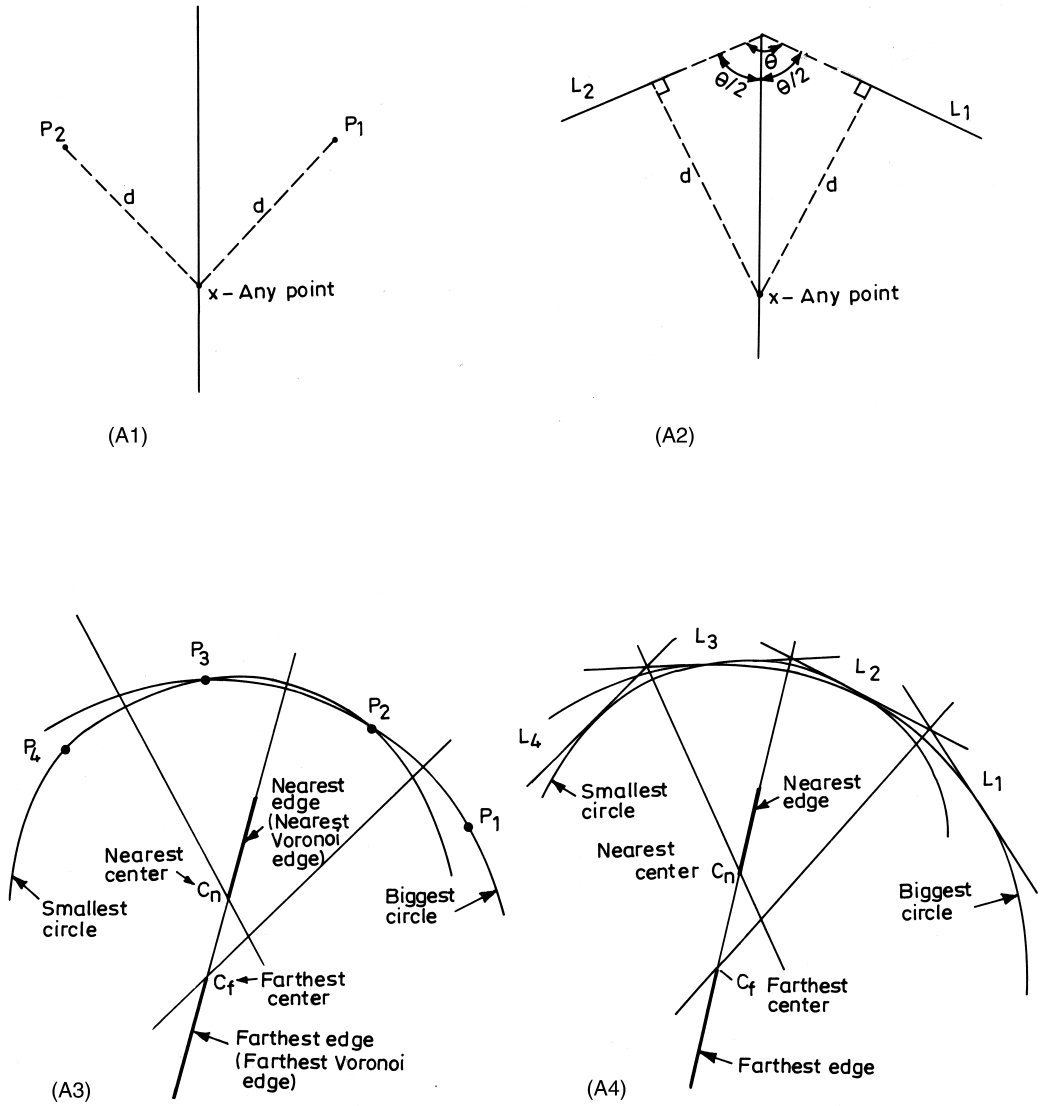

Fig. A. A1: Equi-distant (ED) line; A2: Equi-angular (EA) line; A3: Equi-distant (ED) diagram; A4: Equi-angular (EA) diagram.

Appendix A: Equi-distant (ED) and Equi-angular (EA) lines

Considering two points, namely P_1 and P_2, the line shown in Fig. A1 is a Equi-distant (ED) line. In other words, any point X on ED-line has distances P_1X and P_2X equal. In the present work, the term Equi-distant line is used, because it represents this geometric property in a fundamental way. With X as a center, if a circle is drawn through the point P_1, the circle will pass through P_2 also. In the present work, an Equi-angular (EA) line, which bisects the angle formed by two lines; namely, L_1 and L_2, as shown in Fig. A2, also finds an important application. Interestingly, the perpendicular distances from any point X on this EA-line to lines L_1 and L_2 are equal. If a circle is drawn with X as its center and tangent to L_1, the circle will also be tangential to L_2. Fig. A3 shows the farthest and nearest centers based on equidistant lines. The farthest center results in the biggest circle passing through P_1, P_2, and P_3. Any point away from C_f and along the farthest edge, taken as a cener can yield a circle passing through two points, in this case P_2 and P_3. The line beyond C_f is also known as Farthest Voronoi Edge. In the same way, the line from C_n as shown in Fig. A3 is the nearest (Voronoi) edge. For the equi-angular lines, the farthest center results in the biggest circle tangential to L_1, L_2, and L_3 as shown in Fig. A4. Along the line beyond the farthest center C_f, the circle drawn will be tangential to L_2 and L_3.

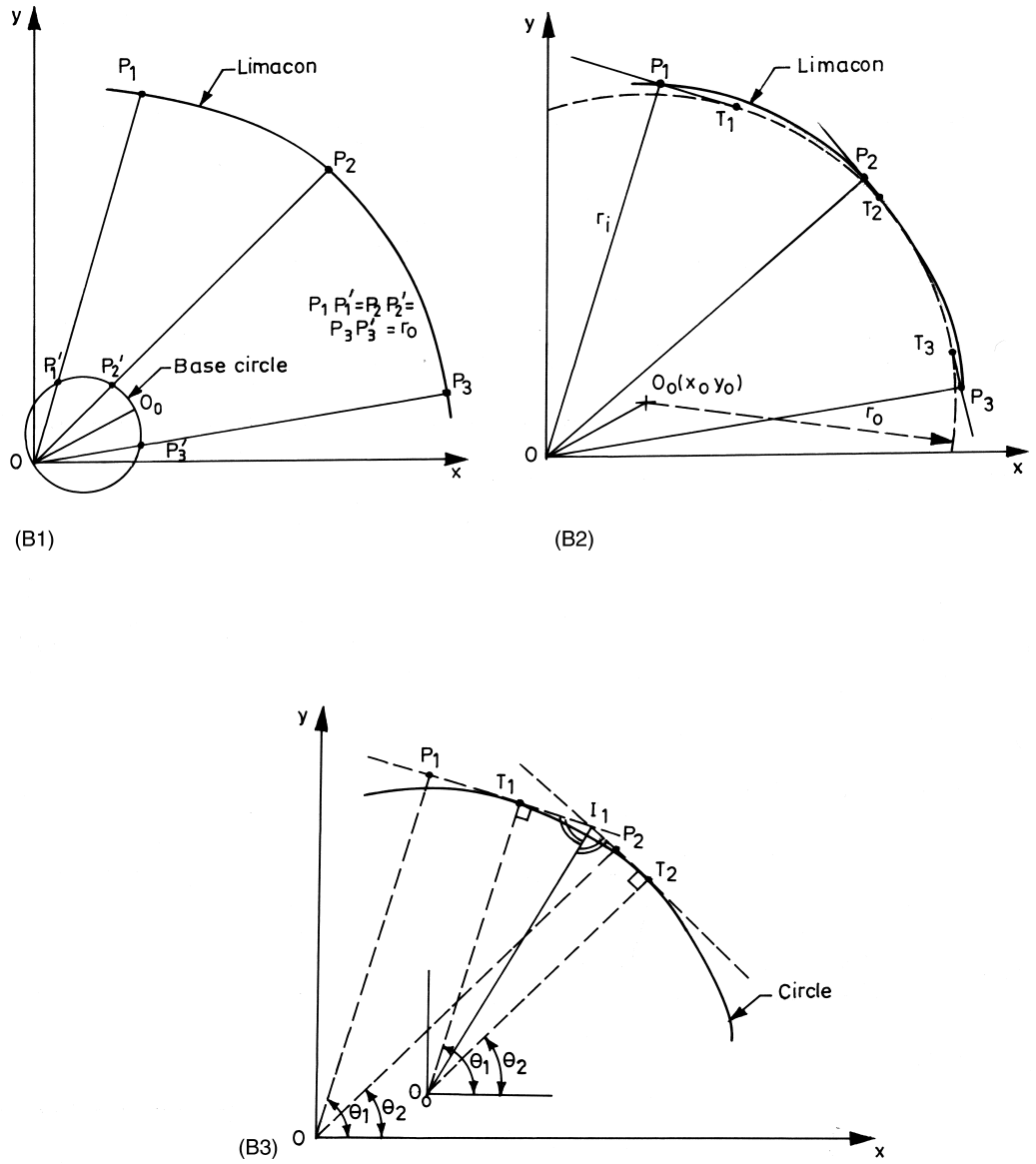

Fig. B. B1: Limacon from a given circle of radius r_0; B2: Limacon from a given circle of radius r_0; B3: Important properties of Limacon.

Appendix B: A Note on Limacon

A limacon has a pole O and an axis OO_o. There are two ways of constructing a limacon geometrically. In Fig. B1, a base circle is drawn with OO_o as its diameter and a line is drawn from the pole O. This line intersects the circle, say, at P_1' and a pont P_1 is located on this line such that the segment $P_1' P_1$ is equal to r_o. By laying out the points P_2, P_3, etc. in a similar manner, a limacon is obtained as a curve passing through these points.

Alternatively, a circle of radius r_o is drawn with a O_o as its center, as shown in Fig. B2. Foot of the perpendicular drawn from the pole O to the tangent of this circle lies on the limacon. Certain interesting properties of the limacon can be seen in Fig. B3. The perpendiculars darwn to the lines OP_1 and OP_2 intersect at I_I. It can be seen that the normals at T_1 and T_2 subtend an angle $\lfloor T_1O_oT_2$ at O_o. By geometry, it is seen that the line I_1O_o bisects the angles $\lfloor T_1O_oT_2$ and $\lfloor P_1I_1P_2$. Also the angle subtended by the normals O_oT_1 and O_oT_2 is equal to the angle between OP_1 and OP_2.

Table C1
Data set 1

C1(a): CMM Data*

Sl. No.	x_i mm	y_i mm
1	65.0038 (7573)	30.0000 (0000)
2	57.6809 (9976)	47.6809 (9976)
3	40.0000 (0000)	55.0041 (1987)
4	22.3181 (7436)	47.6818 (2755)
5	14.9978 (7903)	30.0000 (0000)
6	22.3207 (0923)	12.3207 (0923)
7	40.0000 (0000)	5.0001 (2112)
8	57.6784 (6298)	12.3215 (3797)

*Simulated to match data set C1(b); digits within parentheses are considered for improved accuracy in form evaluation

C1(b): Form Data [3]

Sl. No.	r_i (μm)	θ_i (deg.)
1	4	0
2	4	45
3	3	90
4	5	135
5	2	180
6	3	225
7	1	270
8	2	315

Table C2
Data set 2

C2(a): CMM Data [18]

Sl. No.	x_i mm	y_i mm
1	70.0150	50.0000
2	68.7900	58.4734
3	65.4060	65.9372
4	59.5675	72.7493
5	51.3791	77.7452
6	44.7944	79.6013
7	40.8903	79.9958
8	32.0312	78.9306
9	27.2296	77.1385
10	20.3993	72.7076
11	16.1556	68.2304
12	12.7184	62.4905
13	10.6380	56.0806
14	10.0183	49.2149
15	11.4275	40.8264
16	14.1050	34.8682
17	18.8168	28.7427
18	24.6321	24.2200
19	31.6833	21.1862
20	39.1626	20.0207
21	45.5204	20.5021
22	55.3996	24.2692
23	62.3561	30.0114
24	67.3540	37.6492
25	69.6190	45.2028

Table C2 *(continued)*

C2(b): Form Data*

Sl. No.	r_i (μm)	θ_i (deg.)
1	42.5173	0.0174
2	41.3988	16.4203
3	24.3585	32.1216
4	43.7024	49.3210
5	28.0847	67.7185
6	29.1711	80.8153
7	52.1145	88.3132
8	52.782	105.4077
9	38.3151	115.2042
10	42.5173	130.7984
11	60.1041	142.5940
12	49.0629	155.3895
13	27.6287	168.2855
14	32.6533	181.4823
15	46.8601	197.7795
16	27.4535	210.2785
17	42.5173	225.0787
18	42.8477	239.1802
19	17.3805	253.8828
20	16.3081	268.3867
21	34.0605	280.5907
22	10.0000	300.898
23	12.1482	318.2045
24	37.4254	335.7106
25	31.1207	350.8152

*Obtained by transformation of data set C2(a)

Appendix C

Appendix D List of symbols

x_i, y_i	Cartesian coordinates of *i*th point
r_i, θ_i	Polar coordinate of a point
x_0, y_0	Estimated coordinates of center of the assessment feature
r_0	Radius of assessment circle
e_i	Deviation of *i*th point form assessment feature
e_{max}, e_{min}	Maximum and minimum deviations of the profile
Δ	Circularity error
r_a	Radius of the assumed circle
r_i'	Radius of the points on inverted profile
r_{max}, r_{min}	Maximum and minimum radii
δ	Increment
k	Constant, from 0.5 to 1.0

References

[1] ANSI/ASME Y14.5M. Dimensioning and Tolerancing. New York: American National Standards Institute; The American Society of Mechanical Engineers, 1982.
[2] ISO/R 1101-1983. Technical drawings—Geometrical tolerancing—Guidelines, ISO, Geneva, 12–01.
[3] Shunmugam MS. On assessment of geometric errors. Int J Product Res 1986: 24(2):413–25.
[4] Shunmugam MS. Criteria for computer-aided form evaluation. J Eng Ind 1991;113:233–40.
[5] Murthy TSR, Abdin SZ. Minimum zone evaluation of surfaces. Int J Machine Tool Design Res 1980;2:123–36.

[6] Chetwynd DG. Applications of linear programming to engineering metrology. Proc Inst Mech Eng (Lond) 1985;199(B2):93–100.
[7] Danish P, Shunmugam MS. An algorithm for form error evaluation using the theory of discrete and linear Chebyshev approximations. Comput Meth Appl Mech Eng 1991;92:309–24.
[8] Etesami F, Hong Q. Analysis of two-dimensional measurement data for Automated inspection. J Manufact Syst 1990;9(1):21–34.
[9] Roy UR, Zhang X. Establishment of a pair of concentric circles with the minimum radial separation for assessing roundness error. Comp-Aided Design 1992; 24(3):161–8.
[10] Roy UR, Zhang X. Development and application of voronoi diagrams in the assessment of roundness error in an industrial environment. Computers in industrial engineering 1994;26(1):11–26.
[11] Novasaki O, Barczak ALC. Utilization of voronoi diagrams for circularity algorithms. Prec Eng 1997;20(3):188–95.
[12] Weill R. Tolerancing for function. Ann CIRP 1988;37(2);603–10.
[13] Namboothiri VNN, Shunmugam MS. Function-oriented form evaluation of engineering surfaces. Prec Eng 1998;22(3):98–109.
[14] Weckenmann A, Eitzert H, Garmer M, Weber H. Functionality oriented evaluation and sampling strategy in coordinate metrology. Prec Eng 1995; 17(4): 244–52.
[15] Shunmugam MS. Comparison of linear and normal deviations of form of engineering surfaces. Prec Eng 1987; 9(2):96–102.
[16] Preparata FP, Shamos MI. Computational Geometry: An Introduction. New York: Springer-Verlag, 1985.
[17] Preparata FP, Hong SJ. Convex hulls of finite sets of points in two and three dimensions. Comm ACM 1977; 20(2):87–93.
[18] Namboothiri VNN. Development of algorithms and stratagies for the evaluation of engineering surfaces. Ph. D Thesis, Indian Institute of Technology, Madras, India 1998.